

Paper

Int'l J. of Aeronautical & Space Sci. 16(3), 347–359 (2015)
DOI: <http://dx.doi.org/10.5139/IJASS.2015.16.3.347>

IJASS
International Journal of
Aeronautical and Space Sciences

Rovibrational Energy Transitions and Coupled Chemical Reaction Modeling of $H+H_2$ and $He+H_2$ in DSMC

Jae Gang Kim*

Department of Aerospace System Engineering, Sejong University, Seoul 05006, Korea

Abstract

A method of describing the rovibrational energy transitions and coupled chemical reactions in the direct simulation Monte Carlo (DSMC) calculations is constructed for $H(^2S)+H_2(X^1\Sigma_g)$ and $He(^1S)+H_2(X^1\Sigma_g)$. First, the state-specific total cross sections for each rovibrational states are proposed to describe the state-resolved elastic collisions. The state-resolved method is constructed to describe the rotational-vibrational-translational (RVT) energy transitions and coupled chemical reactions by these state-specific total cross sections and the rovibrational state-to-state transition cross sections of bound-bound and bound-free transitions. The RVT energy transitions and coupled chemical reactions are calculated by the state-resolved method in various heat bath conditions without relying on a macroscopic properties and phenomenological models of the DSMC. In nonequilibrium heat bath calculations, the state-resolved method are validated with those of the master equation calculations and the existing shock-tube experimental data. In bound-free transitions, the parameters of the existing chemical reaction models of the DSMC are proposed through the calibrations in the thermochemical nonequilibrium conditions. When the bound-free transition component of the state-resolved method is replaced by the existing chemical reaction models, the same agreement can be obtained except total collision energy model.

Key words: State-resolved method, RVT energy transition, Nonequilibrium Chemical Reaction, DSMC

1. Introduction

The direct simulation Monte-Carlo (DSMC) [1] is a powerful numerical method for investigating strong thermochemical nonequilibrium flows in a rarefied region. An important part of the DSMC in simulating the nonequilibrium rarefied flows is the physical models employed in describing the elastic and inelastic collisions. Most physical models to describe the thermochemical nonequilibrium in DSMC are of phenomenological nature, and these models describe the inelastic collisions and chemical reactions at the macroscopic level.

In the previous DSMC works [2-6], chemical reactions were described at the microscopic level for atom-molecule collisions by using the results of quasi-classical trajectory (QCT) calculations of the bound-free transitions. However, these models are insufficient: the chemical reactions are dominantly affected by the thermal nonequilibrium of rotational and

vibrational modes induced by the state-to-state kinetics. Also, in the previous master equation studies of H_2 [7, 8], it was found that the rotational-vibrational-translational (RVT) energy transitions have an important role in thermochemical nonequilibrium. These phenomena cannot be fully accounted for in these previous DSMC works because the Larsen-Borgnakke (LB) model [1] adopted in the previous works has a limitation in describing the RVT energy transitions and it has a phenomenological nature and simulates the energy transitions depend on the macroscopic properties.

The purpose of the present work is to construct the state-resolved method to describe the RVT energy transitions and coupled chemical reactions for $H(^2S)+H_2(X^1\Sigma_g)$ and $He(^1S)+H_2(X^1\Sigma_g)$ without relying on a macroscopic properties and phenomenological models of the DSMC. Toward this end, the state-specific total cross sections are proposed for each rovibrational states of H_2 . In the state-resolved method, the

This is an Open Access article distributed under the terms of the Creative Commons Attribution Non-Commercial License (<http://creativecommons.org/licenses/by-nc/3.0/>) which permits unrestricted non-commercial use, distribution, and reproduction in any medium, provided the original work is properly cited.

© * Assistant Professor, Corresponding author: jaegkim@sejong.ac.kr

RVT energy transitions and coupled chemical reactions are described by the state-to-state transition probabilities of the bound-bound and bound-free transitions. These transition probabilities are defined by dividing the rovibrational state-to-state transition cross sections by the state-specific total cross sections. The state-to-state transition cross sections are taken from the existing work by Kim et al. [7]. By using the state-resolved method, the DSMC calculations including the RVT energy transitions and coupled chemical reactions are carried out in various heat bath conditions. The results of rotational and vibrational temperatures and number densities obtained from the DSMC calculations are compared with the results of the master equation calculations and shock tube experimental data [9, 10]. In bound-free transitions, the parameters of the existing chemical reaction models [2, 11-13] of the DSMC are proposed through the calibrations in the nonequilibrium heat bath conditions. The DSMC calculations are performed by the existing chemical reaction models where the bound-bound transitions are treated by the state-resolved method to accurately describe the RVT energy transitions.

2. State-specific Total Cross Sections

Previously, variable hard-sphere (VHS) [1], variable soft-sphere (VSS) [14, 15], general hard-sphere (GHS) [16], and general soft-sphere (GSS) [17, 18] models were developed to determine the total cross sections in the DSMC calculations. However, these previous models have limitations to be employed in the state-resolved method. One of the limitations is that the previous total cross section models are depend on macroscopic properties. The collision parameters of the previous total cross section models are determined at the macroscopic level by the curve-fit of the transport properties and collision integrals. The other limitation is that these models assume that the total cross section depends only on the relative translational energy between colliding particles. This assumption is valid in low temperature gases where the high rovibrational states of molecules are not excited. When the high rovibrational states are excited, however, this assumption is not valid. This is because at highly excited states, the inter-nuclear distance of the colliding molecules increases and significantly influences the total cross section. The state-specific total cross sections to overcome the limitations of the previous total cross section models were initially proposed for the N_2 nonequilibrium work by Kim and Boyd [19]. In this work, it was shown that the state-specific total cross section can accurately describe the thermochemical

nonequilibrium of N_2 in comparing with the results of the VHS and VSS models.

In the present work, this state-specific total cross sections are extended to H_2 . The state-specific total cross sections for each rovibrational states in atom-molecule collisions are defined as follows:

$$\sigma_T(v, j, E_{tr}) = \int_{b=0}^{b_{\max}} \int_{\theta=0}^{\pi} \int_{\phi=0}^{2\pi} \int_{R=\rho^-}^{\rho^+} \int_{\eta=0}^{2\pi} P(E_{tr}, b, \theta, \phi, R, \eta) f_b(b) f_{\theta}(\theta) f_{\phi}(\phi) f_R(R) f_{\eta}(\eta) db d\theta d\phi dR d\eta \quad (1)$$

where σ_T is total cross section, v and j are vibrational and rotational states, respectively. E_{tr} is relative translational energy, b is impact parameter, θ and ϕ is Euler angle, R is inter-nuclear distance of molecule, η is rotational phase angle, f is distribution function for each variables. Also, P is the probability of collisions: it is unity when collision occurs, as zero when it does not occur. For atom-atom collisions, the state-specific total cross sections are defined as

$$\sigma_T(E_{tr}) = \int_{b=0}^{b_{\max}} \int_{\theta=0}^{\pi} \int_{\phi=0}^{2\pi} P(E_{tr}, b, \theta, \phi) f_b(b) f_{\theta}(\theta) f_{\phi}(\phi) db d\theta d\phi \quad (2)$$

Detailed description about the state-specific total cross sections are provided in the work by Kim and Boyd [19]. In the present work, Eqs. (1) and (2) are calculated by the QCT method based on the exact potential energy surfaces by Boothroyd et al. [20, 21] for H+H, H+He, H+ H_2 and He+ H_2 collision pairs. A stratified sampling is employed in obtaining the impact parameter. All the other parameters are selected through the Monte-Carlo method in the QCT calculations. The quasi-bound states are determined by the effective potential method proposed by Kuntz [22]. A total of 3,000 trajectories are calculated per impact parameter with a batch size of 0.1 Å. To ensure convergence of the cross sections, the calculations are performed until all collisions have the non-zero scattering angle.

The state-specific total cross sections of the present work are compared with the VHS model. The total cross sections of the VHS model are determined as

$$\sigma_{T_{VHS}}(E_{tr}) = \sigma_{T_{ref}} \frac{(kT_{ref} / E_{tr})^{\omega-0.5}}{\Gamma(5/2 - \omega)} \quad (3)$$

where k is Boltzmann constant, T_{ref} is reference temperature, and $\sigma_{T_{ref}}$ and ω are the reference total cross sections and viscosity index, respectively. In the present work, the reference total cross sections of the VHS model for atom-molecule and atom-atom collisions are determined as

$$\sigma_{T_{ref}}(T_{ref}) = 4\pi \int_0^{\infty} \frac{\sum_{v,j} \sigma_T(v, j, E_{tr}) Q(v, j, T_{ref})}{\sum_{v,j} Q(v, j, T_{ref})} \left(\frac{m_r}{2\pi kT_{ref}} \right)^{3/2} \exp\left(-\frac{E_{tr}}{kT_{ref}} \right) g^3 dg \quad (4)$$

$$\sigma_{T_{ref}}(T_{ref}) = 4\pi \int_0^\infty \sigma(E_{tr}) \left(\frac{m_r}{2\pi k T_{ref}} \right)^{3/2} \exp\left(-\frac{E_{tr}}{k T_{ref}}\right) g^3 dg \quad (5)$$

respectively. In Eqs. (4) and (5), Q is molecular partition function [23], g is relative speed, and m_r is reduced mass. Another collision parameter ω of Eq. (3) is determined from the relation between the viscosity coefficients and temperature.

$$\mu = \frac{5}{16} \frac{\sqrt{\pi m_r k T}}{\Omega^{(2,2)}} \propto T^\omega \quad (6)$$

where $\Omega^{(2,2)}$ is collision integral and T is equilibrium temperature. The collision integral $\Omega^{(2,2)}$ are taken from the works of Stallcop et al. [24] and Park et al. [25]. The reference total cross sections and viscosity index evaluated in the present work are tabulated in Table 1.

In Fig. 1, the state-specific total cross sections for the atom-atom collisions are compared with the VHS model. In this figure, the differences between the state-specific total cross sections and the VHS model are negligible. This is because

the state-specific total cross sections are dependent only on the collision energy in atom-atom collisions.

In Fig. 2, the state-specific total cross sections for the atom-molecule collision are compared with the VHS model for various vibrational states in rotational $j=0$ and

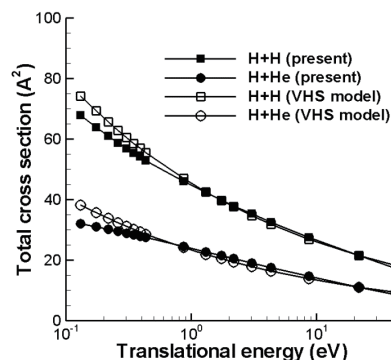


Fig. 1. Comparison of the total cross sections for H+H and He+H collisions between the state-specific total cross sections and the VHS model.

Table 1. Collision parameter and reference total cross sections for the VHS model.

	Collision parameter ω	Reference total cross section (cm^2), $T_{ref}=2,000K$
H+H	0.7415	6.387×10^{-15}
H+He	0.7416	3.291×10^{-15}
H+H ₂	0.8732	5.438×10^{-15}
He+H ₂	0.7953	4.319×10^{-15}

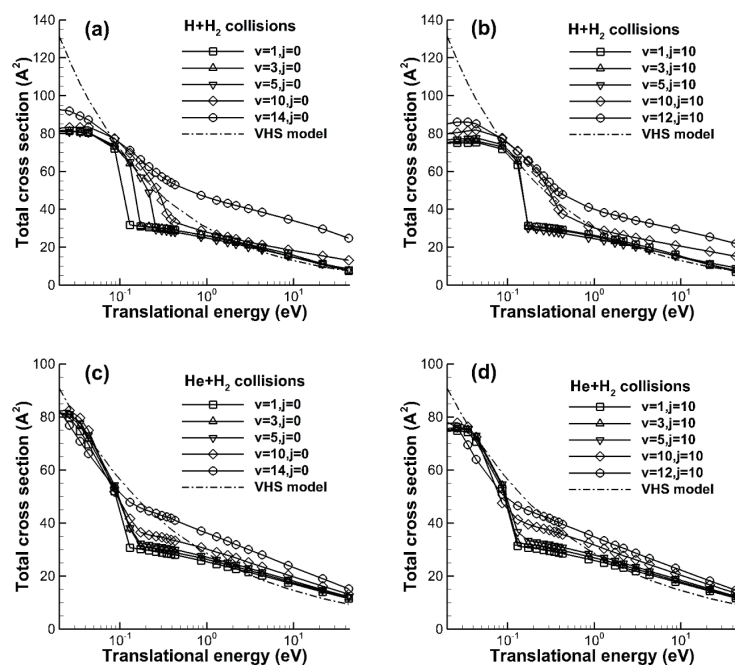


Fig. 2. Comparison of the total cross sections of H+H₂ and He+H₂ for various vibrational states between the state-specific total cross sections and VHS model: (a) H+H₂($v=1, 3, 5, 10, j=0$), (b) H+H₂($v=1, 3, 5, 10, j=10$), (c) He+H₂($v=1, 3, 5, 10, j=0$), (d) He+H₂($v=1, 3, 5, 10, j=10$).

$j=10$. At the same translational energy, the state-specific total cross sections have different cross sections for each vibrational state. This is because the inter-nuclear distance of molecules affects the total cross sections in heavy-particle collisions. These features are discernably shown at the high translational energies and high vibrational states. In comparing with the VHS model, the differences of the total cross sections are discernably shown at the vibrational states $v > 5$ and translational energy $E_{tr} > 1$ eV. In this energy region, most of the dissociation of H_2 are occurred by coupling with the rovibrational states of H_2 [7, 8], and the state-specific total cross sections can accurately describe the nonequilibrium chemical reactions.

In Fig. 3, the state-specific total cross sections for the atom-molecule collision are compared with the VHS model for various rotational states in vibrational $v=0$ and $v=4$. In this figure, the differences of the total cross sections for the various rotational states are negligible. These results of Figs 2 and 3 shows that the inter-nuclear distance of molecules in each rotational and vibrational state affects the total cross section in heavy-particle collisions and the total cross section is mostly dependent on the vibrational states of the molecule. In the previous thermochemical nonequilibrium studies of N_2 , the same result was also observed in that the state-specific total cross sections of N_2 are mostly depend on the vibrational states [19].

In Fig. 4, the transition probabilities of the bound-bound

and bound-free transitions by the state-specific total cross sections are compared with those probabilities by the VHS model for various vibrational states at $E_{tr}=1$ eV. The transition probabilities of the state-specific total cross sections are determined as

$$P(v, j \rightarrow v', j', E_{tr}) = \frac{\sigma(v, j \rightarrow v', j', E_{tr})}{\sigma_T(v, j, E_{tr})} \quad (7)$$

$$P(v, j \rightarrow c, E_{tr}) = \frac{\sigma(v, j \rightarrow c, E_{tr})}{\sigma_T(v, j, E_{tr})} \quad (8)$$

respectively. In Eqs. (7) and (8), $\sigma(v, j \rightarrow v', j', E_{tr})$ and $\sigma(v, j \rightarrow c, E_{tr})$ are the rovibrational state-to-state transition cross sections, and these cross sections are obtained from the work by Kim et al. [7, 8]. In this work, the state-to-state cross sections were obtained from the atomistic calculations of QCT method based on the complicated potential energy surfaces [20, 21]. The bound-bound and bound-free transition probabilities of the VHS model are determined as

$$P_{VHS}(v, j \rightarrow v', j', E_{tr}) = \frac{\sigma(v, j \rightarrow v', j', E_{tr})}{\sigma_{T_{VHS}}(E_{tr})} \quad (9)$$

$$P_{VHS}(v, j \rightarrow c, E_{tr}) = \frac{\sigma(v, j \rightarrow c, E_{tr})}{\sigma_{T_{VHS}}(E_{tr})} \quad (10)$$

respectively. In comparisons of the transition probabilities between the state-specific total cross sections and VHS

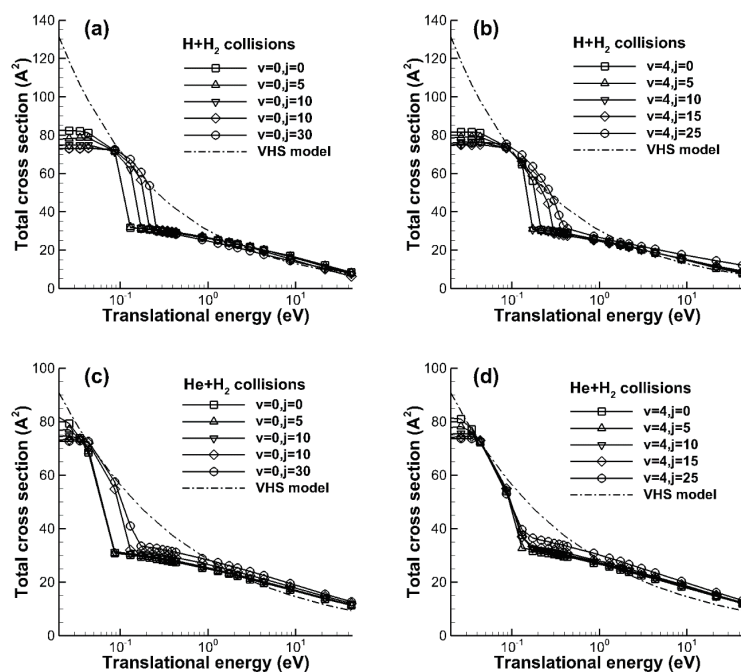


Fig. 3. Comparison of the total cross sections of $H+H_2$ and $He+H_2$ for various rotational states between the state-specific total cross sections and VHS model: (a) $H+H_2(v=0, j=0, 5, 10, 30)$, (b) $H+H_2(v=4, j=0, 5, 10, 30)$, (c) $He+H_2(v=0, j=0, 5, 10, 30)$, (d) $He+H_2(v=4, j=0, 5, 10, 30)$.

model, the difference is only produced by the difference of the total cross sections. In Fig. 4 the transition probabilities of the bound-bound and bound-free transitions for H+H₂ and He+H₂ are presented. The differences between the state-specific total cross sections and VHS model are almost twice for bound-bound transitions, and the differences of the transition probabilities of the bound-free transitions are increased in proportion to the vibrational state of H₂. These results show that the state-specific total cross sections are more adequate to accurately describe the RVT energy transitions and coupled chemical reactions in highly excited rovibrational states.

3. RVT Energy Transitions and Coupled Chemical Reactions in DSMC

In most of the previous DSMC studies [2-6], the phenomenological model of Larsen-Borgnakke [1] was adopted to describe the rotational-translational (RT) and vibrational-translational (VT) transitions. However, in the H₂ molecule, the rovibrational states are fully coupled [7, 8] and the RVT energy transitions have an important role in describing the thermochemical nonequilibrium of H₂, and the LB model has a limitation in describing the RVT energy transitions [19]. In the present work, the state-resolved method to describe the RVT energy transitions

and coupled chemical reactions for H+H₂ and He+H₂ is constructed without relying on a macroscopic properties and phenomenological models of the DSMC.

In the state-resolved method of bound-bound transitions, the state-to-state transition probabilities of the atom-molecule collisions are determined as

$$P_{BB}(v, j \rightarrow v', j', E_{tr}) = \int_{v_0}^{v'} dv'' \int_{j_0}^{j'} dj'' \frac{\sigma(v, j \rightarrow v'', j'', E_{tr})}{\sigma_T(v, j, E_{tr})} \quad (11)$$

In the rovibrational state-to-state transition cross sections, the micro-reversibility [26] is adopted in the endoergic direction as

$$\sigma(v_1, j_1 \rightarrow v_2, j_2, E_{tr}) s_1 m_1 E_{tr} = \sigma(v_2, j_2 \rightarrow v_1, j_1, E_{tr}) s_2 m_2 E_{tr} \quad (12)$$

where s is a statistical multiplicity [23]. The transition probabilities of bound-free transitions from a rovibrational state to the continuum state is determined as

$$P_{BF}(v, j \rightarrow c, E_{tr}) = \frac{\sigma(v, j \rightarrow c, E_{tr})}{\sigma_T(v, j, E_{tr})} \quad (13)$$

By using Eqs. (11) and (13), the RVT energy transitions and coupled chemical reactions of the state-resolved method are constructed for the DSMC calculations.

In order to exactly describe the RVT energy transitions and coupled chemical reactions by the state-resolved method, the initial chemical equilibrium composition and

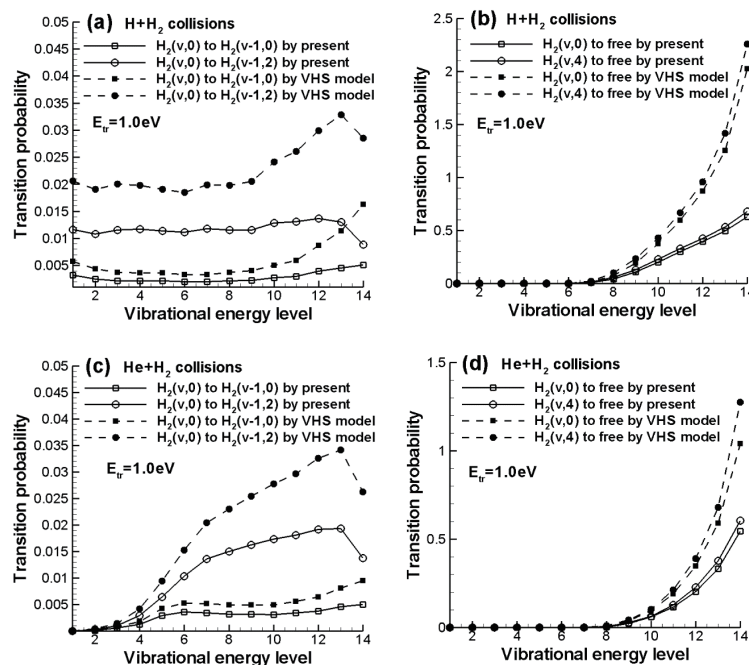


Fig. 4. State-to-state transition probability by the state-specific total cross section (Present) and VHS model for various vibrational states at 1.0 eV: (a) bound-bound transitions of H+H₂, (b) bound-free transitions of H+H₂, (c) bound-bound transitions of He+H₂, (d) bound-free transitions of He+H₂.

the initial rovibrational number density distributions of H_2 are important. In the present work, the initial chemical equilibrium composition for a given initial temperature is evaluated by Saha equation [23] of rovibrational states including the exact rovibrational energies of H_2 calculated by the quantum mechanical method [7, 8]. For the initial rovibrational number density distributions of H_2 , the exact rovibrational populations based on the atomic and molecular partition functions are employed through the acceptance-rejection method [19] in the present work.

In Fig. 5(a), at the equilibrium temperatures of 3,000 K, 5,000 K, and 10,000 K, the distributions of normalized number densities are compared with the exact partition function relations for various vibrational states. 100,000 particles are generated to make the distribution curve in the DSMC calculations. In Fig. 5(a), the distributions of initial molecules agree with those of the partition functions. In Fig. 5(b), the distributions of normalized number density for various rotational states of $H_2(v=0, 1, 3, 5, \text{ and } 8)$ are compared with the exact partition functions for the equilibrium temperature of 5,000 K. As shown in Fig. 5(b), the rotational distributions are accurately reproduced by the DSMC calculations in comparing with those of the exact partition functions.

The RVT energy transitions and coupled chemical reactions of the state-resolved method are studied in isothermal heat bath conditions. A zero-dimensional DSMC code with some manipulations is employed in the present work. In the DSMC calculations, 100,000 particles are generated. The initial number density of H_2 is $1.0 \times 10^{18} \text{ cm}^{-3}$, and those of H and He are both $5.0 \times 10^{17} \text{ cm}^{-3}$. The initial nonequilibrium conditions of seven heating cases are tabulated in Table 2. In the DSMC calculations, it is assumed that the rovibrational energy excitations and chemical reactions occur at a constant volume and isothermal condition.

In validating the state-resolved method in nonequilibrium heat bath conditions, the rovibrational master equation

calculations of $H+H_2$ and $He+H_2$ are adopted. In these master equation calculations, the rovibrational state-to-state transition rate coefficients are obtained from the work by Kim et al. [7, 8], which is the same reference database of the rovibrational state-to-state transition cross sections used in the state-resolved method of the DSMC calculations. Details about the master equation calculations are provided in the work by Kim et al. [7, 8].

In Fig. 6, the rotational and vibrational temperature relaxations calculated by the state-resolved method are compared with the relaxations of the master equation calculations for $H+H_2$ and $He+H_2$. In the present work, the energy-equivalent method [7, 8] is employed to determine the rotational and vibrational temperatures in DSMC and master equation calculations. For Cases 3 to 6, the temperature relaxation curves of the DSMC calculations by state-resolved method are almost identical to those of the master equation calculations. These results show that the microscopic and deterministic calculations of the state-resolved method can accurately describe the RVT energy transitions.

In Fig. 7, the rotational and vibrational relaxation parameters for $H+H_2$ and $He+H_2$ evaluated by the state-resolved method are compared with the shock-tube experimental data by Dove and Teitelbaum [9]. In this experiment, a laser Schlieren technique was adopted in measuring the relaxation time of incident shock waves

Table 2. Initial heat bath conditions for $H+H_2$ and $He+H_2$ mixtures.

	T	$T_r = T_v$
Case 1	1,000K	2,000K
Case 2	1,000K	3,000K
Case 3	1,000K	4,000K
Case 4	1,000K	6,000K
Case 5	1,000K	8,000K
Case 6	1,000K	10,000K
Case 7	1,000K	16,000K

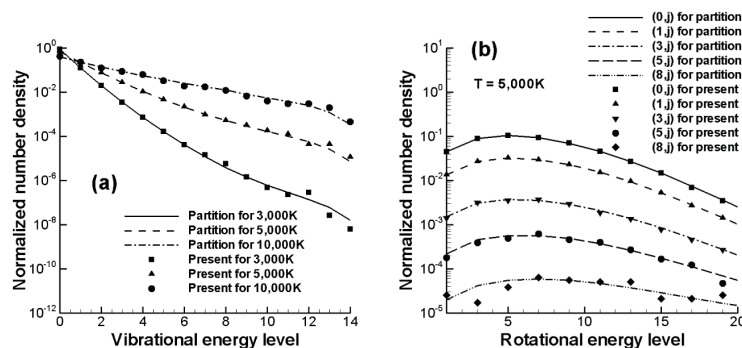


Fig. 5. Comparison of the initial normalized number density distributions between the state-resolved method (Present) and exact partition functions: (a) $H_2(v=0 \text{ to } 14)$ at $T=3,000 \text{ K}, 5,000 \text{ K}, \text{ and } 10,000 \text{ K}$, (b) $H_2(v=0, 1, 3, 5, 8, j)$ at $T=5,000 \text{ K}$.

at a temperature range between 1,350 K and 3,000 K. The rotational and vibrational energy relaxations evaluated by the state-resolved method can be described by the Landau-Teller type of energy relaxation equation [28] as

$$\frac{\partial e_r}{\partial t} = \frac{e_r(T) - e_r(T_r)}{\tau_r} \quad (14)$$

$$\frac{\partial e_v}{\partial t} = \frac{e_v(T) - e_v(T_v)}{\tau_v} \quad (15)$$

where τ_r and τ_v are rotational and vibrational relaxation times, respectively. In the present work, the relaxation times

of the state-resolved method are determined by the e-folding curve-fit method proposed by Kim et al. [7, 8]. By multiplying τ_r and τ_v by pressure, one obtains the characteristic rotational and vibrational relaxation parameters $p\tau_r$ and $p\tau_v$, respectively. In Fig. 7, the vibrational relaxation parameter of He+H₂ by the state-resolved method is compared with the experimental data, and it agrees well with the measured value. In He+H₂, the rotational relaxation occurs faster than vibrational relaxation for all test cases. The rotational relaxation time approaches the vibrational relaxation time above 16,000 K. In the temperature relaxations of H+H₂, the rotational and vibrational relaxations occur similarly for all

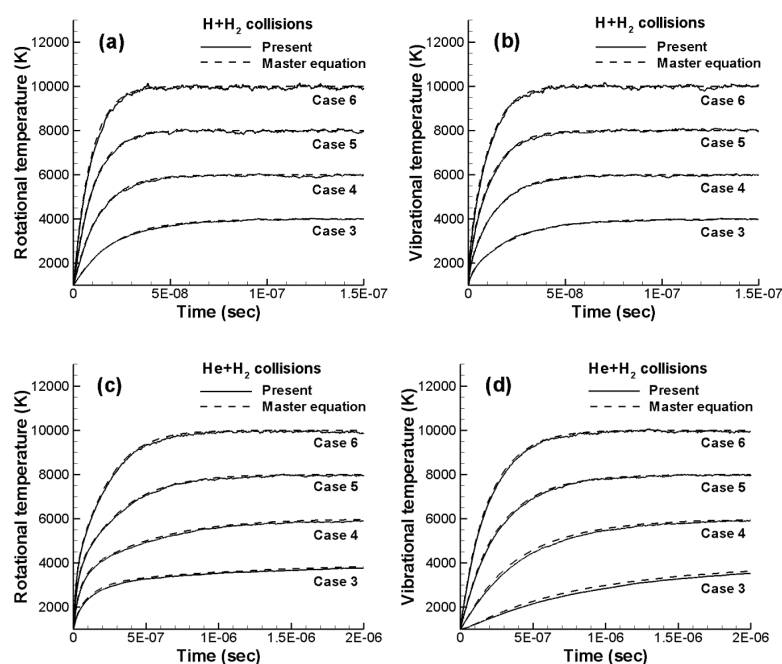


Fig. 6. Comparison of the rotational and vibrational temperature relaxations between the state-resolved method and master equation calculations: (a) rotational temperature relaxation for H+H₂, (b) vibrational temperature relaxation for H+H₂, (c) rotational temperature relaxation for He+H₂, (d) vibrational temperature relaxation for He+H₂.

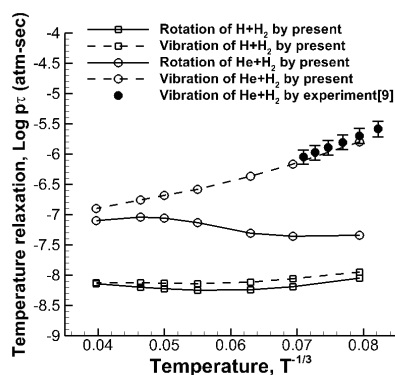


Fig. 7. Comparison of the rotational and vibrational relaxation parameters between the state-resolved method and the shock-tube experimental data [9].

test cases. These phenomena are more obvious for the cases with the initial equilibrium temperature higher than 10,000 K, even though overall relaxation patterns of the rotational and vibrational temperatures are similar for all test cases considered.

In Fig. 8, the rotational and vibrational temperature and number density relaxations evaluated by the state-resolved method are compared with those by the master equation calculations. For Cases 4 to 7, the rotational and vibrational temperatures and number density relaxations of the state-resolved method agree well with the results of master equation calculations before statistical fluctuation appear. These fluctuations of the temperatures of Case 7 result from the dissociation of H₂. For both H and He collisions,

a rovibrational quasi-steady state (QSS) period is observed. During this rovibrational QSS period, the rotational and vibrational temperatures are almost constant, and the number density of dissociated H atom increases rapidly. In the QSS period, the number density rate of change of rotational and vibrational states is much smaller than both the sum of all incoming rates and sum of all outgoing rates by nonequilibrium chemical reactions [19]. This phenomenon results in the rotational and vibrational energies maintaining near-constant values. Most of the nonequilibrium chemical reactions coupled with the RVT energy transitions occur in the QSS period. In comparing of the state-resolve method and the master equation calculations of Fig. 8, such QSS phenomena is obviously shown in the DSMC calculations by the state-resolved method.

In Fig. 9, the number density distributions evaluated by the state-resolved method for Case 6 are compared with those of the master equation calculations at the QSS time point of 5.0×10^{-8} s and 1.0×10^{-6} s for $H+H_2$ and $He+H_2$, respectively. In Figs. 11(a) and 11(c), comparison is made for the various rotational state, and in Figs. 12(b) and 12(d), it is made for vibrational states. At the QSS time point where the nonequilibrium chemical reactions are dominant, the number density distributions of the state-resolved method and the master equation calculations are almost identical

for various rotational and vibrational states. These results show that the thermochemical nonequilibrium of $H+H_2$ and $He+H_2$ are accurately described by the state-resolve method in the DSMC calculations.

In Fig. 10, the chemical reaction rate coefficients calculated in the state-resolved method for Cases 1 to 7 are compared with the experimental reference values by Cohen and Westberg [10]. In the reaction rate coefficients, the experimental results are available only in the temperature range between 1,000 K and 5,000 K. The figure shows that the chemical reaction rate coefficients by the state-resolved method agree very well with the experimental values. These results show that the state-resolved method can accurately describe the nonequilibrium chemical reactions which are dominantly occurred in the QSS conditions.

4. Nonequilibrium Calibration of the Previous Chemical Reaction Models

In the present work, the nonequilibrium chemical reactions are calculated additionally by using the previous chemical reaction models [2, 11-13] of the DSMC. The purpose of this calculations is to see whether the existing models are compatible with the nonequilibrium distributions of the rovibrational states. Total collision energy (TCE)

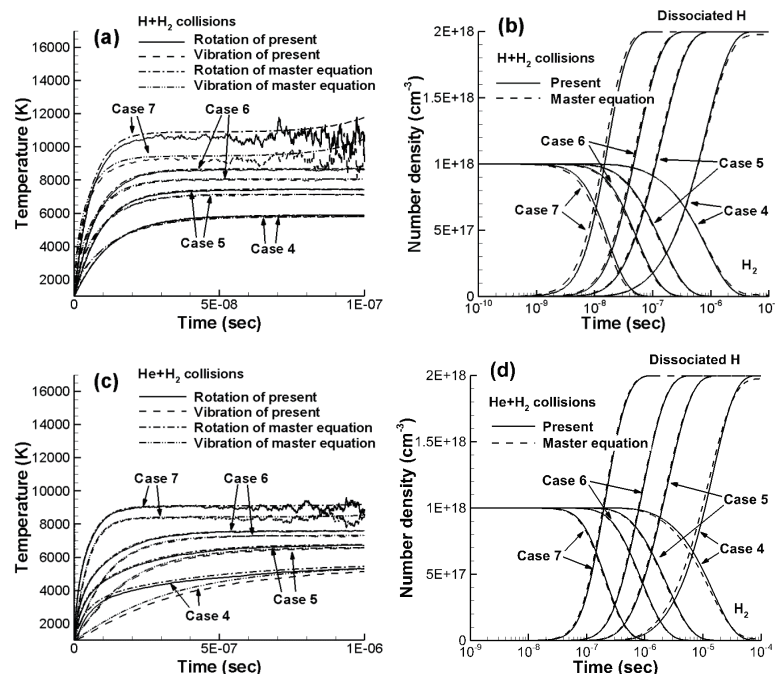


Fig. 8. Comparison of the rotational and vibrational temperatures and number density relaxations between the state-resolved method and the master equation calculations for Cases 4 to 7: (a) rotational and vibrational temperature relaxations of $H+H_2$, (b) number density relaxations of $H+H_2$, (c) rotational and vibrational temperature relaxations of $He+H_2$ mixture, (d) number density relaxations of $He+H_2$.

model [11], vibrational favored dissociation (VFD) model [12], weak vibrational biased rotation (WVBr) model [2], and full threshold (FT) model [13] are adopted in describing the nonequilibrium chemical reactions of H+H₂ and He+H₂. In the present work, the bound-bound transition is treated by the state-resolved method in order to accurately describe the RVT energy transitions because the nonequilibrium chemical reactions of H₂ is mainly coupled with the RVT energy transitions [7, 8]. The bound-free transition part of the state-resolved method is substituted by the TCE, VFD, WVBr, and FT models.

In previous chemical reaction models, the VFD, WVBr,

and FT models treat the chemical reactions as the rotational or vibrational energy coupled transitions, and such coupled transitions are described by arbitrary parameters. Therefore, the chemical reaction parameters of the previous DSMC models need to be calibrated. In the previous DSMC works [3, 4, 11-13], these parameters were calibrated in the equilibrium heat bath conditions. However, the calibration in the equilibrium conditions is questionable because the chemical reactions are occurred in the thermochemical nonequilibrium status of the QSS. In order to accurately describe the nonequilibrium chemical reactions, the parameters of the previous DSMC models need to be

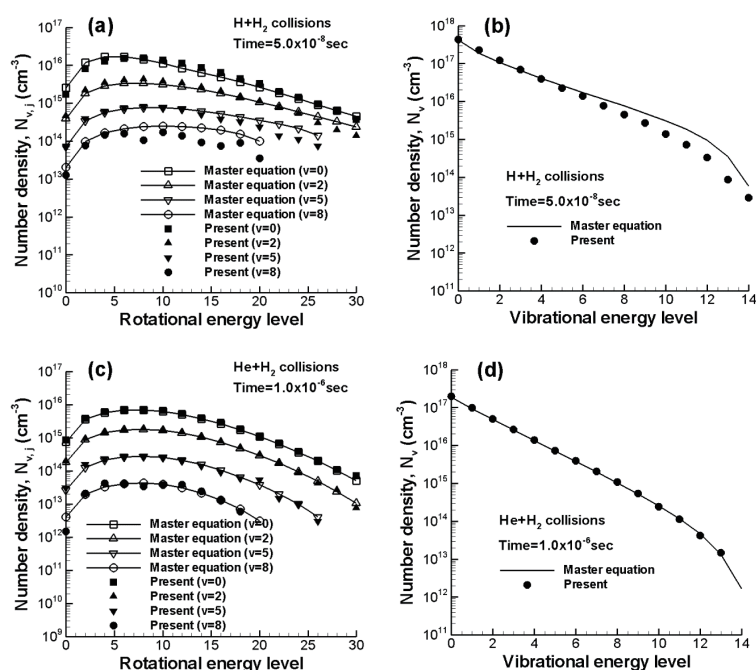


Fig. 9. Comparison of the number density distribution at the QSS time point between the state-resolved method and the master equation calculations: (a) various rotational states of H+H₂(v=0, 2, 5, 8, j), (b) various vibrational states of H+H₂(v=0 to 14), (c) various rotational states of He+H₂(v=0, 2, 5, 8, j), (d) various vibrational states of He+H₂(v=0 to 14).

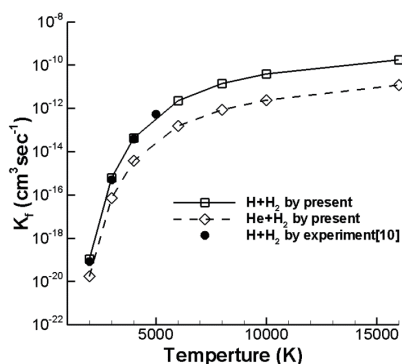


Fig. 10. Comparison of chemical reaction rate coefficients between the state-resolved method and the experimental reference values [10].

calibrated in the nonequilibrium status including the QSS. In the present work, the calibration of the chemical reaction parameters is carried out in the nonequilibrium heat bath conditions evaluated by the master equation calculations, where the RVT energy transitions, coupled chemical reactions, and rovibrational QSS of energy transitions are accurately describe by the state-to-state kinetics of H+H₂ and He+H₂.

In Fig. 11, the sample calibration of the chemical reaction parameter ϕ_{VFD} of the VFD model for H+H₂ is presented. For Case 4, the number density relaxation evaluated by the master equation calculations is positioned between the results of the DSMC calculations of $\phi_{VFD}=7$ and $\phi_{VFD}=9$. For Case 5, the results is positioned between $\phi_{VFD}=5$ and

$\phi_{VFD}=7$. For Case 6, $\phi_{VFD}=3$ and $\phi_{VFD}=5$. Also for Case 7, it is position between $\phi_{VFD}=1$ and $\phi_{VFD}=3$. In order to determine the chemical reaction parameter ϕ_{VFD} for each test cases, a linear interpolation method is adopted. Then, the parameter ϕ_{VFD} have 7.9658, 5.3616, 4.1028, and 2.5987 for Case 4 to 7,

respectively.

The chemical reaction parameters of the VFD, WVBr, and FT models for $H+H_2$ and $He+H_2$ are calibrated by using the same methodology presented in Fig. 11. These parameters are tabulated in Table 3. In these calibration processes,

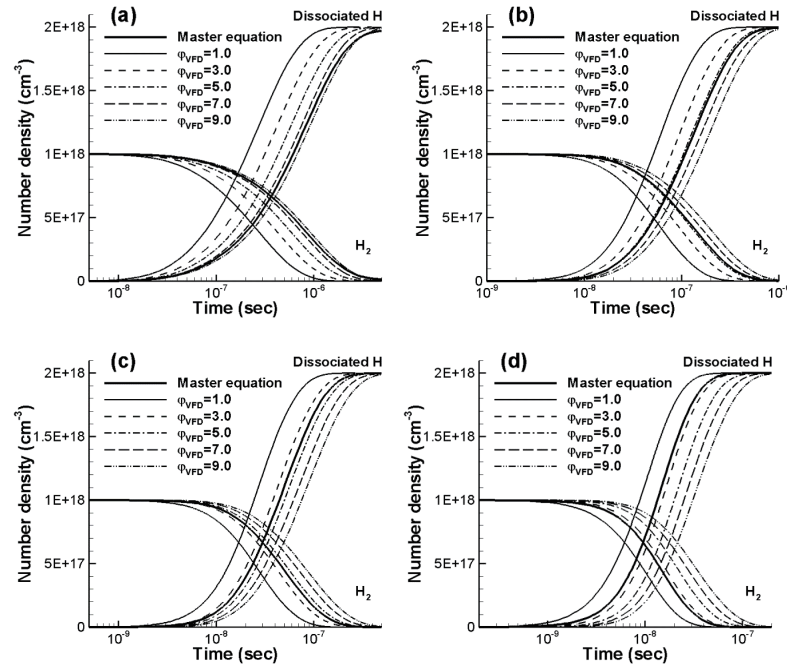


Fig. 11. Sample calibrations of the chemical reaction parameter of the VFD model for $H+H_2$ in nonequilibrium conditions: (a) Case 4, (b) Case 5, (c) Case 6, (d) Case 7.

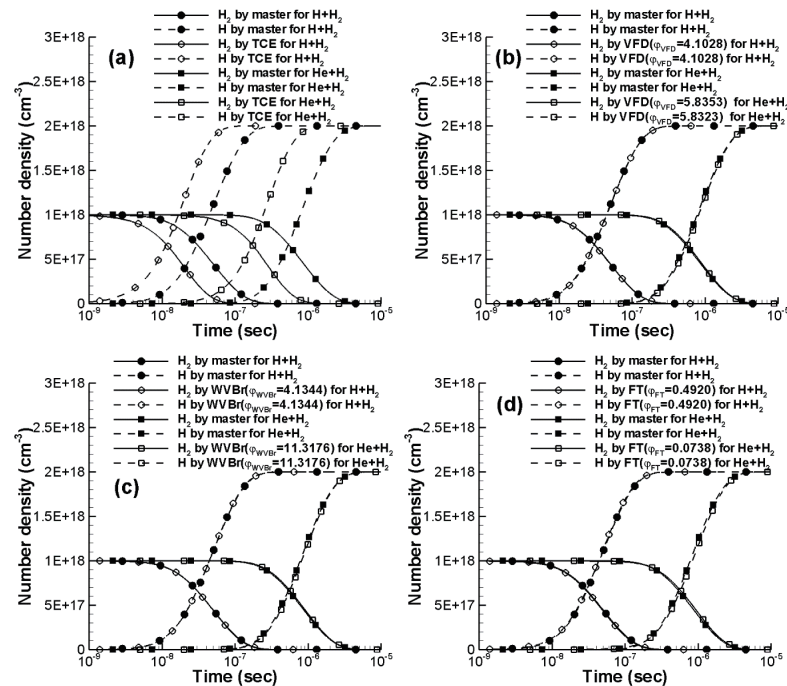


Fig. 12. Comparison of the number density relaxations between the previous DSMC chemical models and the master equation calculations for $H+H_2$ and $He+H_2$: (a) TCE model, (b) VFD model, (c) WVBr model, (d) FT model.

the reference number density relaxations are evaluated by the master equation calculations in order to calibrate the parameters as nonequilibrium status.

In Fig. 12, the number density relaxations calculated by the previous DSMC chemical reaction models [2, 9-11] are compared with the results of master equation calculations for the nonequilibrium heat bath conditions of Case 6. In the DSMC calculations, the bound-bound transitions are treated by the state-resolved method, and only the bound-free transition component of the state-resolved method is replaced by the existing chemical reaction models. In Fig. 12, the number density relaxation patterns of the previous DSMC chemical reaction models of VFD, WVBr, and FT models are in agreement with the results of the master equation calculations. However, discernible differences are observed in the TCE model even though the RVT energy transitions are accurately described through the state-resolved method. This is because the TCE model does not include the nonequilibrium adapted parameters, and results

show that the TCE model has a limitation in describing the nonequilibrium chemical reactions.

In Fig. 13, the rotational and vibrational number density distributions evaluated by the previous DSMC chemical reaction models of the TCE, VFD, WVBr, and FT models are compared with those of the master equation calculations at the QSS time point of 5.0×10^{-8} s and 1.0×10^{-6} s for H+H₂ and He+H₂, respectively. In Figs. 13(a) and 13(c), the comparison is made for the various rotational states of vibrational $v=0$. In Figs. 13(b) and 13(d), the number density is compared for the various vibrational states of rotational $j=0$. Except for the TCE model, the number density distributions for H+H₂ and He+H₂ have distributions similar to those of the master equation calculations. These results show that the previous DSMC chemical reaction models of the VFD, WVBr, and FT models, where the chemical reaction parameters are calibrated in the nonequilibrium conditions, are enough to describe the nonequilibrium chemical reactions of H+H₂ and He+H₂.

Table 3. Calibrated dissociation parameters of the previous DSMC dissociation models.

	H+H ₂			He+H ₂		
	VFD	WVBr	FT	VFD	WVBr	FT
Case 4	7.9678	5.8969	0.68700	10.758	14.896	0.14521
Case 5	5.3616	4.7550	0.57075	7.5365	12.695	0.10054
Case 6	4.1028	4.1344	0.49199	5.8323	11.318	0.073797
Case 7	2.5987	3.3928	0.32755	3.2553	8.6934	0.047205

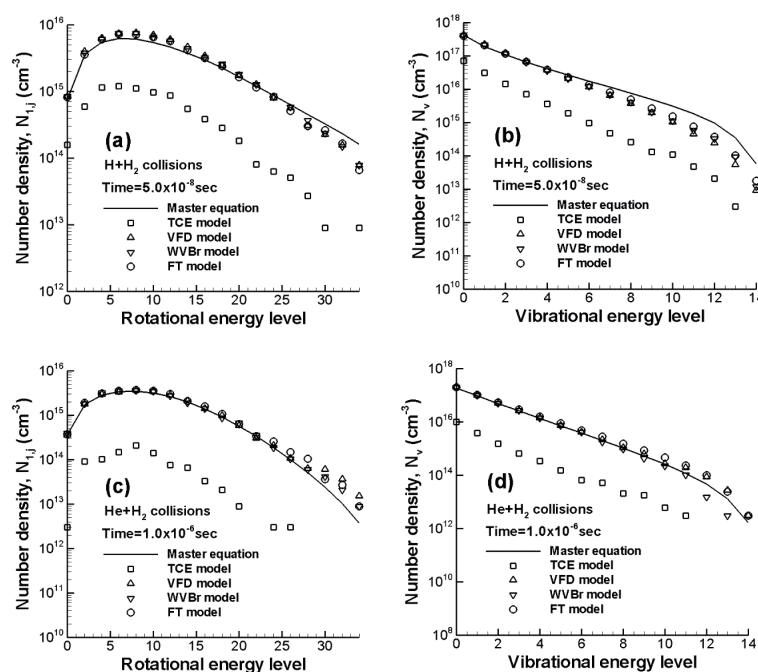


Fig. 13. Comparison of the number density distribution at the QSS time point between the previous DSMC chemical reaction models and the master equation calculations: (a) various rotational states of H+H₂($v=0, j$), (b) various vibrational states of H+H₂($v=0$ to 14, $j=0$), (c) various rotational states of He+H₂($v=0, j$), (d) various vibrational states of He+H₂($v=0$ to 14, $j=0$).

5. Conclusions

Direct simulation Monte Carlo (DSMC) calculations for $H+H_2$ and $He+H_2$ are performed by a state-resolved method in which the elastic and inelastic collisions are described at the microscopic level of cross sections using a deterministic method without macroscopic and phenomenological assumptions. In the present work, the state-specific total cross sections of $H+H_2$ and $He+H_2$ for each rovibrational states are derived. Unlike the previous total cross section models, in the state-specific total cross sections, the internuclear distance of colliding molecules is considered in determining the cross sections. The state-specific total cross sections are evaluated through the quasi-classical trajectory method based on the exact potential energy surfaces of $H+H_2$ and $He+H_2$. The state-resolved method is constructed using the state-specific total cross sections and the rovibrational state-to-state transition cross sections obtained from the work by Kim et al. [7, 8] in order to accurately describe the rotational-vibrational-translational (RVT) energy transitions and coupled chemical reactions. This first principles approach avoids use of any phenomenological assumptions and macroscopic properties. In nonequilibrium heat bath calculations, the results of DSMC calculations by the state-resolved method are compared with those of master equation calculations. The rotational and vibrational nonequilibrium including the RVT energy transitions are exactly described by the state-resolved method. For the nonequilibrium chemical reactions, the state-resolved method accurately describes the quasi-steady state (QSS) of rotational and vibrational energies and the nonequilibrium chemical reactions in this QSS period. The nonequilibrium energy relaxations and the chemical reactions are compared with the shock-tube experimental data and are in agreement with the reference values. When the bound-free transitions of the state-resolved method are replaced by the previous DSMC chemical reaction models with the calibration of the chemical reaction parameters in the nonequilibrium conditions, it is found that the vibrational favored dissociation model, weak vibrational biased rotation model, and full threshold model are enough to describe the nonequilibrium chemical reactions of $H+H_2$ and $He+H_2$. However, the total collision energy (TCE) model has limitations in describing the nonequilibrium chemical reaction.

Acknowledgements

The author gratefully acknowledges funding for this work through Sejong University Research Grant 20150235.

References

- [1] Bird, G. A., *Molecular Gas Dynamics and Direct Simulation of Gas Flows*, Clarendon, Oxford, 1994.
- [2] Koura, K., "A Set of Model Cross Sections for the Monte Carlo Simulation of Rarefied Real Gases: Atom-diatom Collisions", *Physics of Fluids*, Vol. 6, No. 10, 1994, pp. 3473-3486.
- [3] Boyd, I. D., Bose, D. and Candler, G. V., "Monte Carlo Modeling of Nitric Oxide Formation Based on Quasi-classical Trajectory Calculations", *Physics of Fluids*, Vol. 9, No. 4, 1997, pp. 1162-1170.
- [4] Wadsworth, D. C. and Wysong, I. J., "Vibrational Favoring Effect in DSMC Dissociation Models", *Physics of Fluids*, Vol. 9, No. 12, 1997, pp. 3873-3884.
- [5] Gimelshein, S. F., Ivanov, M. S., Markelov, G. N. and Gorbachev, Y. E., "Statistical Simulation of Nonequilibrium Rarefied Flows with Quasiclassical Vibrational Energy Transfer Models", *Journal of Thermophysics and Heat Transfer*, Vol. 12, No. 4, 1998, pp. 489-495.
- [6] Ozawa, T., Levin, D. A. and Wysong, I. J., "Chemical Reaction Modeling for Hypervelocity Collisions between O and HCl", *Physics of Fluids*, Vol. 19, No. 5, 2007, article 056102.
- [7] Kim, J. G., Kwon, O. J. and Park, C., "Master Equation Study and Nonequilibrium Chemical Reactions for $H+H_2$ and $He+H_2$ ", *Journal of Thermophysics and Heat Transfer*, Vol. 23, No. 3, 2009, pp. 443-453.
- [8] Kim, J. G., Kwon, O. J. and Park, C., "Master Equation Study and Nonequilibrium Chemical Reactions for Hydrogen Molecule", *Journal of Thermophysics and Heat Transfer*, Vol. 24, No. 2, 2010, pp. 281-290.
- [9] Dove, J. E. and Teitelbaum, H., "The Vibrational Relaxation of H_2 , I: Experimental Measurement of the Rate of Relaxation by H_2 , He, Ne, Ar and Kr", *Chemical Physics*, Vol. 6, No. 3, 1974, pp. 431-444.
- [10] Cohen, N. and Westberg, K. R., "Chemical Kinetic Data Sheets for High-Temperature Chemical Reactions", *Journal of Physical Chemistry Reference Data*, Vol. 12, No. 3, 1983, pp. 531-1267.
- [11] Bird, G. A., "Monte-Carlo Simulation in An Engineering Context", *Rarefied Gas Dynamics*, edited by S. Fisher, AIAA, New York, 1981, pp. 239-255.
- [12] Haas, B. L. and Boyd, I. D., "Models for Direct Simulation of Coupled Vibration-dissociation", *Physics of Fluids A*, Vol. 5, No. 2, 1993, pp. 478-489.
- [13] Boyd, I. D., "A Threshold Line Dissociation Model for the Direct Simulation Monte Carlo Method", *Physics of Fluids*, Vol. 8, No. 5, 1996, pp. 1293-1300.
- [14] Koura, K. and Matsumoto, H., "Variable Soft Sphere Molecular Model for Invers-power-law or Lennard-Jones Potential", *Physics of Fluids A*, Vol. 3, No. 10, 1991, pp. 2459-

2465.

[15] Koura, K. and Matsumoto, H. "Variable Soft Sphere Molecular Model for Air Species", *Physics of Fluids A*, Vol. 4, No. 5, 1992, pp. 1083-1085.

[16] Hassan, H. A. and Hash, D. B., "A General Hard Sphere Model for Monte Carlo Simulation", *Physics of Fluids A*, Vol. 7, No. 3, 1993, pp. 738-744.

[17] Fan, J., "A General Soft-sphere Model for Monte Carlo Simulation", *Physics of Fluids*, Vol. 14, No. 12, 2002, pp. 4399-4405.

[18] Kim, J. G., Kwon, O. J. and Park, C., "Modification and Expansion of the General Soft-sphere Model To High Temperature Based on Collision Integrals", *Physics of Fluids*, Vol. 20, No. 1, 2008, article 017105.

[19] Kim, J. G. and Boyd, I. D., "Monte Carlo Simulation of Nitrogen Dissociation Based on State-Resolved Cross Sections", *Physics of Fluids*, Vol. 26, 2014, article 012006.

[20] Boothroyd, A. I., Keogh, W. J., Martin, P. G. and Peterson, M. R., "A Refined H3 Potential Energy Surface", *Journal of Chemical Physics*, Vol. 104, No. 18, 1996, pp. 7139-7152.

[21] Boothroyd, A. I., Martin, P. G. and Peterson, M. R., "Accurate Analytic He-H2 Potential Energy Surface from

A Greatly Expanded Set of Ab-initio Energies", *Journal of Chemical Physics*, Vol. 119, No. 6, 2003, pp. 3187-3207.

[22] Bernstein, R. B., *Atom-molecule collision theory-a guide for the experimentalist*, Plenum Press, New York and London, 1979.

[23] Park, C., *Nonequilibrium Hypersonic Aerothermodynamics*, John Wiley & Sons, New York, 1990.

[24] Stallcop, J. R., Levin, E. and Partridge, H., "Transport Properties of Hydrogen", *Journal of Thermophysics and Heat Transfer*, Vol. 12, No. 4, 1998, pp. 514-519.

[25] Park, C., Jaffe, R. L. and Partridge, H., "Chemical Kinetic Parameters of Hyperbolic Earth Entry", *Journal of Thermophysics and Heat Transfer*, Vol. 15, No. 1, 2001, pp. 76-90.

[26] Mandy, M. E. and Martin, P. G., "State-to-state Rate Coefficients for H+H₂", *Journal of Chemical Physics*, Vol. 110, No. 16, 1999, pp. 7811-7820.

[27] Park, C., "Thermochemical Relaxation in Shock Tunnels", *Journal of Thermophysics and Heat Transfer*, Vol. 20, No. 4, 2006, pp. 689-698.

[28] Millikan, R. C. and White, D. R., "Systematics of Vibrational Relaxation", *Journal of Chemical Physics*, Vol. 39, No. 12, 1963, pp. 3209-3213.